



Original scientific paper

Synthesis of porous indium phosphide with nickel oxide crystallites on the surface

Yana Suchikova✉, Ihor Bohdanov¹, Sergii Kovachov¹, Andriy Lazarenko¹, Iryna Bardus¹, Alma Dauletbekova², Inesh Kenzhina³ and Anatoli I. Popov^{2,4}

¹Berdyansk State Pedagogical University, Berdyansk, Ukraine

²L. N. Gumilyov Eurasian National University, Nur-Sultan 010008, Kazakhstan

³Kazakh-British Technical University, Almaty 050000, Kazakhstan

⁴Institute of Solid State Physics, University of Latvia, Riga LV-1063, Latvia

Corresponding author: ✉yanasuchikova@gmail.com; Tel.: +38(066)338-78-64

Received: February 15, 2022; Accepted: June 26, 2022; Published: July 6, 2022

Abstract

In this paper, the technology of synthesis of crystallites and nanocrystallites of nickel oxide on the surface of indium phosphide is described. This technology consists of two stages. In the first stage, porous indium phosphide is formed on the surface of a single crystal of indium phosphide. The formation of such a porous layer provides better adhesion to the surface of the sample. The second stage involves the preparation of the solution that contains nickel ions, application of this solution to the surface of porous indium phosphide, followed by annealing. As a result, NiO/NiC₂O₄·2H₂O/por-InP/mono-InP structure was formed. Surface morphological parameters were obtained using scanning electron microscopy and EDX-analysis of chemical composition. Chemical analysis confirmed the partial formation of nickel oxide from nickel oxalate layer by thermal annealing. Using scanning electron microscopy, it has been established that the crystallites have a large scatter in diameter, but they may be divided into three characteristic groups: macro-; meso- and nano-crystallites. Such structures may find prospects for application in electrochemical capacitors and lithium-ion batteries. Further research is needed for methodology improvement to obtain structures with predetermined controlled properties.

Keywords

Nickel oxalate; annealing; electrochemical etching; coating; EDX spectrum

Introduction

Metal oxide semiconductors have recently been widely researched due to the prospects of their application as sensors, lasers, and in a wide range of photon detection and electronic devices, solar energy, etc. [1,2]. Among such types of materials, MgO [3], Al₂O₃ [4], KNbO₃ and LiNbO₃ [5,6], TiO₂ [7,8], ZnO [9] and SnO₂ [10] are the most studied. Thus, zinc oxide was grown using the epitaxial method on ZnSe substrate, as researched in paper [11]. In another paper [12], the authors demonstrated the prospects for the application of SnO₂ to create solar cells.

At present, the great and close attention of many research groups is focused on new materials such as Ga₂O₃ [13,14], ZnGa₂O₄ [15] and BaGa₂O₄ [16]. Among the top prospect materials is also NiO due to its chemical stability and unique electrochemical properties. Nickel oxide has a band gap in the range of 3.6 - 4.0 eV that offers a great value for photovoltaic devices, supercapacitors, sensors, etc. [17,18]. Nickel oxide nanostructures, in particular nanotubes, nanoparticles and nanowires, offer even a greater value [19].

The widely used methods of obtaining nanoparticles and nanostructures of nickel oxide are methods of precipitation, dehydration and oxidation by steam-based etching [20]. However, these methods are usually quite complex and expensive and require special equipment. Therefore, at present, there is a necessity for development of simple and inexpensive methods of nickel oxide synthesis. Another problem in the growth of oxide semiconductors is the choice of substrate. The fact is that crystal lattices mismatch, while the chemical stability of many semiconductors prevents the adhesion to the substrates, significantly affecting the quality of the resulting layers.

In this paper, we research the growth of nickel oxalate (NiC₂O₄·2H₂O) and subsequently crystals of nickel oxide (NiO) on indium phosphide (InP) substrate using a two-stage technology.

Experimental

The structures were formed in two stages. The first stage is the formation of a porous pattern on the surface of monocrystal indium phosphide. This step is necessary for better adhesion to the monocrystalline indium phosphide (mono-InP) substrate of nickel-containing compounds. As it is known, porous layers have fewer dislocations under the surface, which hinders the excess stress [21]. Therefore, such porous layers are considered to be 'soft' substrates, and they are becoming more popular [22]. The second stage is the deposition of nickel oxalate and synthesis of nickel oxide crystallites on the porous surface of InP (por-InP).

Formation of porous layer on mono-InP

The first stage was intended to form pores on the surface of indium phosphide. Monocrystalline high-alloy (S) indium phosphide samples of n-type conductivity with surface orientation (111) were used. Before the experiment, the samples were cleaned, degreased in acetic solution, and dried in a stream of oxygen.

The samples were then electrochemically etched in hydrochloric acid solution in a standard two-electrode electrolytic cell with a platinum cathode. The aqueous-alcoholic solution (C₂H₅OH : H₂O = 1:2) of hydrochloric acid with an acid concentration of 7 % was used as the electrolyte. A few drops of bromic acid were added to the solution. It should be noted that this electrolyte composition is not sufficiently selective for the (111) surface of monocrystalline n-InP. Such choice of electrolyte is conditional on the fact that the task was not to obtain a dense porous layer in this experiment [23,24]. The main purpose was to ensure surface roughness by etching the surface, as well as bulk defects to remove excess crystal stress.

Etching was carried out using the constant voltage of 5 V for 5 min. In the course of etching, a large number of bubbles were observed on the semiconductor wafer. Bubbles shall be the result of oxygen evolution. As a rule, gas bubbles cause disruption of the oxides locally formed on the surface of the semiconductor. In order to reduce the effect of bubble generation, the electrolyte solution was periodically stirred with the use of a mechanical stirrer. Following the etching, the samples were dried in a stream of oxygen for 2 h, washed in deionized water and kept outdoors for 3 days. The

samples became dark gray and lost their full gloss. This provides evidence of texturing of the crystal surface and formation of the extended macroroughness.

Formation of nickel particles on the surface of por-InP

For the purpose of NiO formation, the two-stage method was used, which consisted of the hydrothermal method and annealing. All substances used in this experiment had a high purity class and did not require additional purification.

At the first stage, five portions (mass) of $\text{NiCl}_2 \cdot 6\text{H}_2\text{O}$ were dissolved in a mixture containing two portions of ethylene glycol and one portion of deionized water. The resulting mixture was heated in a beaker to 40 °C. Then, it was stirred with a magnetic stirrer for 20 min. 1 g of $\text{Na}_2\text{C}_2\text{O}_4$ was added to the resulting solution. The resulting suspension was stirred with a magnetic stirrer for 15 min. The purpose of this step was to obtain Ni^+ ions and their homogeneous dispersion in the solution. The resulting suspension was transferred to porous indium phosphide. The samples were heated in a muffle furnace at 230 °C for 3 hours. Then the samples were cooled to room temperature. Following the experiment, the samples were air-dried for 3 months.

The morphology of the obtained structures was researched using SEO-SEM Inspect S50-B scanning electron microscope. The chemical composition was researched by EDX method. The calculation by surface points and mapping technology was applied.

Results and discussion

Figure 1 shows the morphology of the n-InP porous surface following electrochemical etching. Image analysis provides evidence of two types of etching pits, the occurrence of which is conditional on two different mechanisms of electrochemical crystal dissolution.

The first type – massive etched areas that shall be the result of etching at the surface defect location areas. The size of such etching pits in the transverse diameter is 5 μm . It can be seen that such areas are characterized only by surface etching - etching pits do not advance into the depth of the sample, and they grow mainly on the crystal surface.

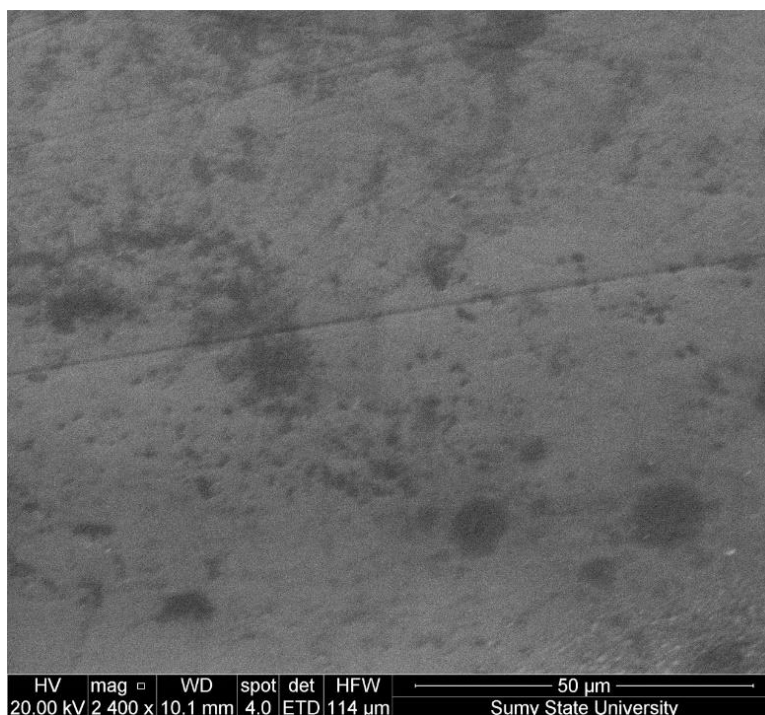


Figure 1. SEM image of the morphology of por-InP porous surface

The second type – so-called ‘seeding pore formation’- is characterized by spontaneous removal of atoms from the crystal surface. Such etching may lead to disruption of the stoichiometric composition of the material as a result of uneven etching of phosphorus and indium lattices. These etching pits form an assembly of small pores on the surface. The average pore diameter varies from 70 to 200 nm. The pores grow to the deep of the crystal in the form of thin parallel channels. The surface porosity is -below 15 %, which characterizes such a structure as a low porosity structure.

As a result of etching, the sample stoichiometry was significantly disrupted (Figure 2 and Table 1). Almost the same concentrations (in atomic units) of indium and phosphorus may be observed. Carbon is also on the surface, it appeared due to the interaction of the sample surface with the electrolyte. In the etching of semiconductors in acid solution, the interphase layers are formed during constant potential superposition at the semiconductor/electrolyte interface (the Gouy-Chapman layer, the Helmholtz layer). The result shall also be the formation of adsorbed species, which may subsequently form stable compounds. Most likely, the presence of carbon is conditional on this mechanism.

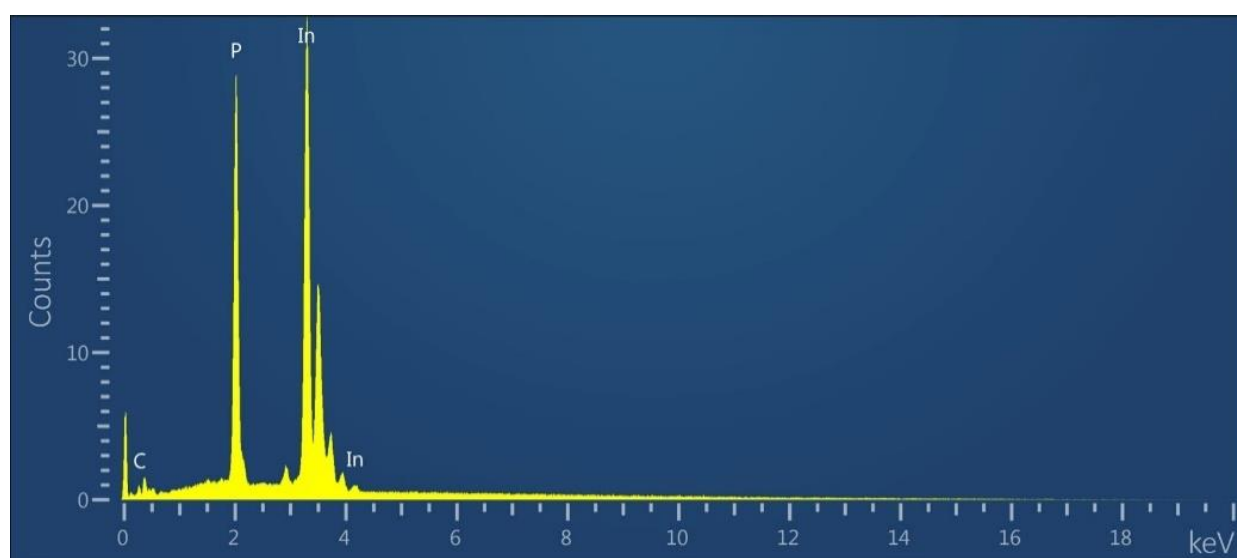


Figure 2. EDX spectrum of por-InP synthesized by electrochemical etching on mono-InP substrate.

Table 1. Elemental composition of por-InP surface by atomic and mass units

Element	Line type	Content, mass%	Content, at.%
P	K series	20.37	40.64
In	L series	76.05	40.92
C	K series	3.58	18.44
Total		100.00	100.00

It should be noted that carbon concentration is quite low (3.58 mass.% and 18.44 at.%, respectively). Therefore, it can be assumed that these compounds will not have a critical effect on the properties of the resulting structure. On the other hand, in order to overcome this phenomenon in the course of electrochemical etching, it is necessary to stir the electrolyte, such stirring will prevent the formation of bubbles near the crystal surface and will allow forming of a clean structure without impurities.

Figure 3 shows the crystal surface following precipitation of nickel-containing suspension and annealing in a muffle furnace. The formation of a solid thin film with crystallites on the surface may be observed. The morphology of the resulting structures demonstrates spherical crystallites of different diameters that tend to agglomerate.

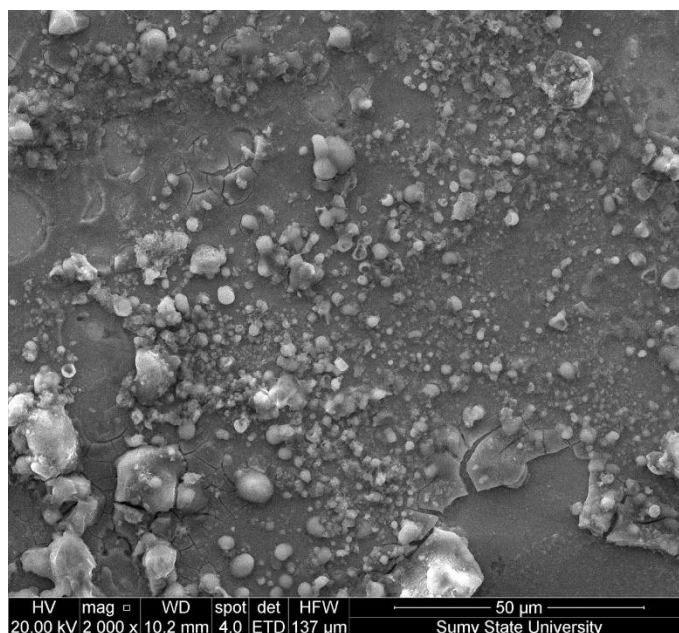


Figure 3. SEM image of por-InP surface with the nickel-containing surface layer

Figure 4 shows EDX mapping of the formed structure surface. It can be concluded that the structure has atoms of indium, phosphorus, oxygen and nickel on the surface. Chlorine and carbon are also present in low concentrations. It can be seen that phosphorus and indium are allocated on the surface almost evenly. These elements are not observed only in the points of concentration of crystallites. The predominant points of oxygen and nickel concentration are crystallites, but they may be observed on the entire surface. Chlorine and carbon are present in small inclusions on the crystal surface.

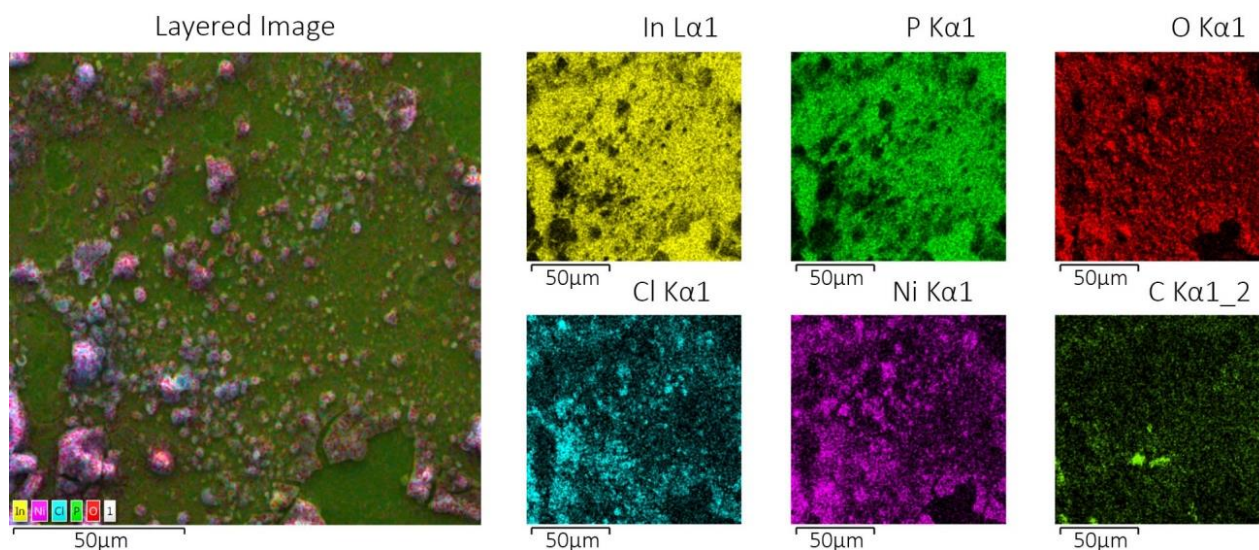


Figure 4. Energy dispersive X-ray (EDX) mapping analysis of the sample

Based on the data obtained (Fig. 4), it can be assumed that the structure consists of a dense layer of nickel oxalate dihydrate ($\text{NiC}_2\text{O}_4 \cdot 2\text{H}_2\text{O}$). Nickel oxalate dihydrate is known to be one of the most important precursors for the synthesis of nickel oxide and pure nickel [25]. For this purpose, nickel oxalate is calcined and dehydrated, resulting in NiO powder [26]. In our case, we used the application of $\text{NiC}_2\text{O}_4 \cdot 2\text{H}_2\text{O}$ solution on the por-InP substrate, resulting in the formation of oxalate containing layer with NiO inclusions (crystallites). Our results are in good agreement with the data previously obtained [27,28]. Note that a similar mechanism of synthesis of NiO nanocrystallites with

$\text{NiC}_2\text{O}_4 \cdot 2\text{H}_2\text{O}$ is demonstrated in the paper [28], with the fundamental difference that the oxalate layer was transferred to the oxide layer within 24 hours.

Figure 5 (a - i) demonstrates the crystallites formed on the film surface. It can be seen that the crystallites tend to agglomerate (Fig. 5 a, b, f). Some of them have open 'windows,' which is evidence of the evaporation of water from them in the course of thermal annealing (b, c, d). Crystallites have a very large scatter in diameter - from 100 nm to 10 μm . In particular, we can distinguish three characteristic dimensions:

- [1] massive crystallites, that are the agglomerates of smaller ones, having a size of 10 - 20 μm (Fig. 5 b, e, f);
- [2] medium crystallites, the size of which is in the range 1 - 5 μm (Fig. 5 a, d, e); they have a characteristic spherical shape or torus shape;
- [3] small crystallites of nanometer size - from 100 to 200 nm (Fig. 5 c, e); such crystallites pack densely on the surface, and they are allocated in the form of islands.

The presence of various types of structures shall be the evidence of evaporation and crystallization process incompleteness. In the event of longer processing periods, the islands will be 'dried out' and crystallized. This argument is also supported by the fact that the crystallites are in the form of nanowires in certain points, it is a characteristic of nickel oxide [29]. Figure 5 (g, h, i) demonstrates the wire structures are formed. Their thickness is 0.5 - 1 μm , and length 2- 3 μm .

Thus, a multilayer structure was formed, it contained 4 basic layers (from bottom to top) (Figure 6):

- [1] a layer of monocrystal InP - virgin crystal, basic 'working' substrate;
- [2] a porous InP layer that was formed by electrochemical etching on mono-InP in order to make the surface rough and to etch defects that are the sources of excessive stress;
- [3] a thin layer of nickel oxalate, $\text{NiC}_2\text{O}_4 \cdot 2\text{H}_2\text{O}$, that was formed on the por-InP surface by application of the solution and annealing;
- [4] an upper layer consisting of NiO crystallites and nanocrystallites that were formed during partial annealing of the nickel oxalate layer.

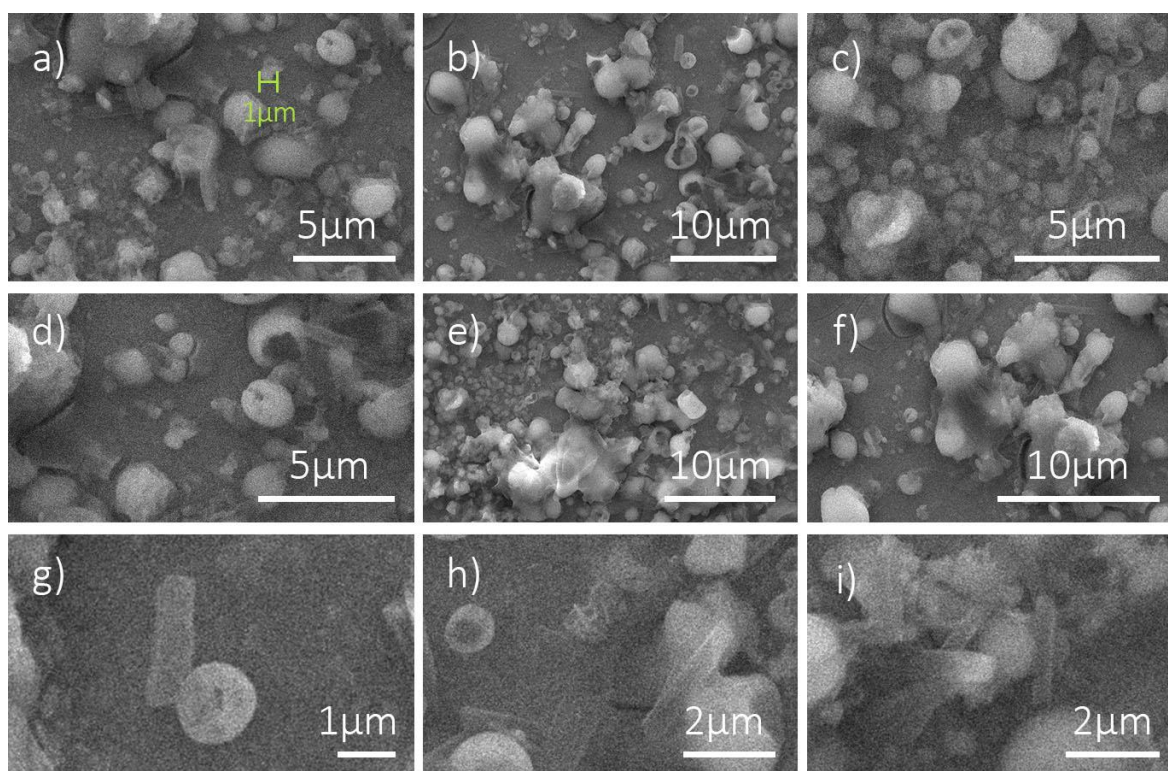


Figure 5. SEM images of NiO crystallites and nanocrystallites

The nickel oxalate layer transformation is evidenced by cracking in some parts of the surface (Figure 7). Due to the aqueous phase drying, it can be seen that the layer becomes brittle, cracked and separated from the surface of porous indium phosphide in these parts. Such behavior is typical and predictable. If annealing is continued for longer, the layer will be separated from the surface. The main problem is the preservation of NiO crystallites on the InP surface. The formation of por-InP on mono-InP allows one to solve this problem partially.

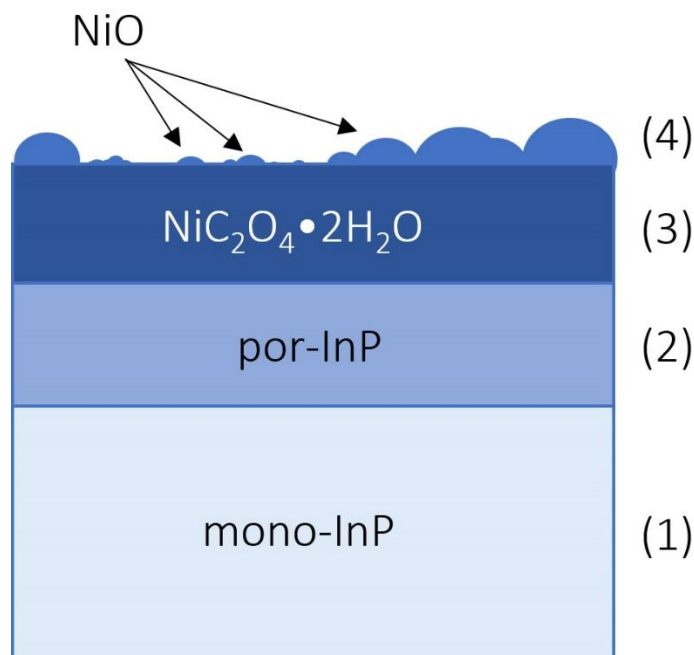


Figure 6. Schematic image of NiO/NiC₂O₄·2H₂O/por-InP/mono-InP structure

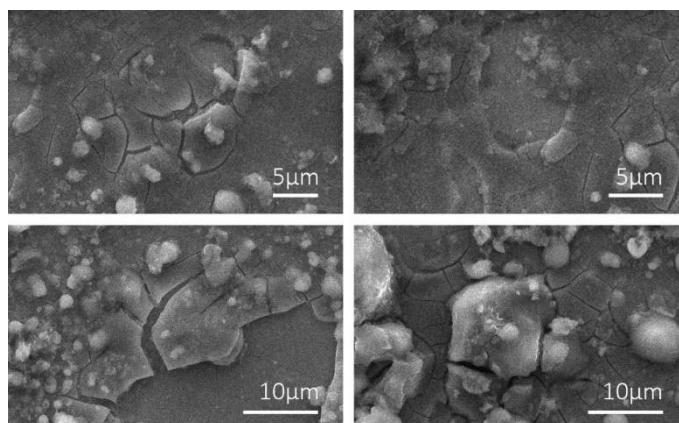


Figure 7. SEM images of NiO/NiC₂O₄·2H₂O/por-InP/mono-InP structure surface

As already mentioned, nickel oxide is a very promising material. Thus, NiO nanoparticles are widely used as anodes for lithium-ion batteries [30], they are also promising for use in electrochemical supercapacitors [31]. Their use as sensitized dyes and as photocathodes have been reported [32]. Electrochemical, magnetic and antibacterial properties are also striking [33]. Therefore, further development of the methods for obtaining nickel oxide nanoparticles is necessary. It should be noted that the first steps of the simple synthesis of crystallites and nickel oxide nanoparticles on porous semiconductor substrates were made in the presented research. The technology requires further improvement, particularly in the removal of the oxalate layer from substrate surface and development of mechanisms that will allow the synthesis of more uniform particles in size, well adhered to the substrate.

Conclusions

The article demonstrates the simple protocol of synthesis of the NiC₂O₄·2H₂O layer with NiO crystallites. The structures were formed on mono-InP substrate that was pre-etched in order to form rough porous layer on the surface. It is demonstrated that the two-stage technology of electrochemical etching of the substrate with subsequent application of nickel oxalate on the surface and annealing allows the formation of a multilayer structure of NiO/NiC₂O₄·2H₂O/por-InP/mono-InP. Provided, however, that NiO is present on the surface in the form of crystallites and nanoparticles. Such structure may find striking applications in modern electronic instrumentation. Further steps should be taken in order to control the shape and the size of nanostructures, which is a common strategy of modern nanophase materials science, and to make decisions on optimization of the productivity and efficiency due to structural dependent properties.

Acknowledgements: Y. Suchikova, S. Kovachov, I. Bohdanov, I. Bardus show their appreciation to the Ministry of Education and Science of Ukraine for its support, in particular: grant 0122U000129 "Search for Optimal Conditions for the Synthesis of Nanostructures on the Surface of Semiconductors A3B5, A2B6 and Silicon for Photonics and Solar Energy," and grant 0121U109426 "Theoretical and Methodological Principles of Systemic Fundamentalization of Intended Specialist Training in the Field of Nanophase Materials Science for Productive Professional Activity".

References

- [1] S. W. Kim, S. Kwon, Y. K. Kim, *Nanomaterials* **11(2)** (2021) 288. <https://doi.org/10.3390/nano11020288>
- [2] L. Yang, J. Wei, Z. Ma, P. Song, J. Ma, Y. Zhao, X. Wang, *Nanomaterials* **9(12)** (2019) 1789. <https://doi.org/10.3390/nano9121789>
- [3] E. Shablonin, A. I. Popov, A. Lushchik, A. Kotlov, S. Dolgov, *Physica B* **477** (2015) 133-136. <https://doi.org/10.1016/j.physb.2015.08.032>
- [4] E. Feldbach, E. Töldsepp, M. Kirm, A. Lushchik, K. Mizohata, J. Räisänen, *Optical Materials* **55** (2016) 164-167. <https://doi.org/10.1016/j.optmat.2019.109308>
- [5] V. Pankratov, D. Millers, L. Grigorjeva, A. O. Matkovskii, P. Potera, I. Pracka, T. Łukasiewicz, *Optical Materials* **22(3)** (2003) 257-262. [https://doi.org/10.1016/S0925-3467\(02\)00285-9](https://doi.org/10.1016/S0925-3467(02)00285-9)
- [6] L. Grigorjeva, D. K. Millers, V. Pankratov, R. T. Williams, R. I. Eglitis, E. A. Kotomin, G. Borstel, *Solid State Communications* **129(11)** (2004) 691-696. <https://doi.org/10.1016/j.ssc.2003.12.031>
- [7] V. Serga, R. Burve, A. Krumina, M. Romanova, E. A. Kotomin, A. I. Popov, *Crystals* **11(4)** (2021) 431. <https://doi.org/10.3390/cryst11040431>
- [8] V. Serga, R. Burve, A. Krumina, V. Pankratova, A. I. Popov, V. Pankratov, *Journal of Materials Research and Technology* **13** (2021) 2350-2360. <https://doi.org/10.1016/j.jmrt.2021.06.029>
- [9] Z. Meng, B. Zhu, Y. Zhang, L. Luo, Y. Zhang, *Chinese Journal of Tissue Engineering Research* **26(22)** (2022) 2095-4344. <https://doi.org/10.12307/2022.277>
- [10] H. Min, D. Y. Lee, J. Kim, G. Kim, K. S. Lee, J. Kim, S. Seok, *Nature* **598(7881)** (2021) 444-450. <https://doi.org/10.1038/s41586-021-03964-8>
- [11] I. V. Rogozin, *Thin Solid Films* **517(15)** (2009) 4318-4321. <https://doi.org/10.1016/j.tsf.2008.12.002>
- [12] H. Min, D. Y. Lee, J. Kim, G. Kim, K. S. Lee, J. Kim, S. Seok, *Nature* **598(7881)** (2021) 444-450. <https://doi.org/10.1038/s41586-021-03964-8>
- [13] A. Luchechko, V. Vasylytsiv, L. Kostyk, O. Tsvetkova, A. I. Popov, *Nuclear Instruments and Methods in Physics Research B* **441** (2019) 12-17. <https://doi.org/10.1016/j.nimb.2018.12.045>

- [14] A. Usseinov, Z. Koishybayeva, A. Platonenko, J. Purans, A. I. Popov, *Materials* **14(23)** (2021) 7384. <https://doi.org/10.3390/ma14237384>
- [15] A. Luchechko, Y. Zhydachevskyy, S. Ubizskii, O. Kravets, A. I. Popov, U. Rogulis, E. Elsts, E. Bulur, A. Suchocki, *Scientific Reports* **9(1)** (2019) 9544. <https://doi.org/10.1038/s41598-019-45869-7>
- [16] H. Klym, I. Karbovnyk, A. Luchechko, Y. Kostiv, V. Pankratova, A. I. Popov, *Crystals* **11(12)** (2021) 1515. <https://doi.org/10.3390/cryst11121515>
- [17] T. T. Le Dang, M. Tonezzer, *Procedia Engineering* **120** (2015) 427-434. <https://doi.org/10.1016/j.proeng.2015.08.658>
- [18] T. N. J. I. Edison, R. Atchudan, Y. R. Lee, *Electrochimica Acta* **283** (2018) 1609-1617. <https://doi.org/10.1016/j.electacta.2018.07.101>
- [19] Z. Alhashem, C. Awada, F. Ahmed, A.H. Farha, *Crystals* **11(6)** (2021) 613. <https://doi.org/10.3390/cryst11060613>
- [20] X. Chen, Y. Zhao, W. Li, X. Zhang, Y. Li, *Optical Materials* **124** (2022) 111959. <https://doi.org/10.1016/j.optmat.2021.111959>
- [21] S. Vambol, I. Bogdanov, V. Vambol, O. Hurenko, S. Onishchenko, *Eastern-European Journal of Enterprise Technologies* **3(5-87)** (2017) 37-44. <https://doi.org/10.15587/1729-4061.2017.104039>
- [22] Y. O. Suchikova, I. T. Bogdanov, S. S. Kovachov, *Archives of Materials Science and Engineering* **98(2)** (2019) 49-56. <https://doi.org/10.5604/01.3001.0013.4606>
- [23] J. A. Suchikova, V. V. Kidalov, G. A. Sukach, *Functional Materials* **17(1)** (2010) 131-134. <http://functmaterials.org.ua/contents/17-1/fm171-24.pdf>
- [24] Ya. A. Suchikova, V. V. Kidalov, G. A. Sukach, *Journal of Nano- and Electronic Physics* **1(4)** (2009) 111-118. https://jnep.sumdu.edu.ua/download/numbers/2009/4/articles/en/jnep_eng_2009_V1_N4_111-118.pdf
- [25] B. R. Shen, H. Shen, Y. X. Pan, T. F. Chen, X. E. Cai, *Zeitschrift für Physikalische Chemie* **2015** (2001) 1413. <https://doi.org/10.1524/zpch.2001.215.11.1413>
- [26] B. Małecka, A. Małecki, E. Drożdż-Cieśla, L. Tortet, P. Llewellyn, F. Rouquerol, *Thermochimica Acta* **466(1-2)** (2007) 57-62. <https://doi.org/10.1016/j.tca.2007.10.010>
- [27] A. A. Najim, F.M. Hassan, H. S. Rasheed, H. Ismail, H.H. Darwoysh, *Optical Materials* **121** (2021) 111602. <https://doi.org/10.1016/j.optmat.2021.111602>
- [28] T. T. L. Dang, M. Tonezzer, V. H. Nguyen, *Journal of Nanomaterials* **2015** (2015) 785856 <https://doi.org/10.1155/2015/785856>
- [29] D.A. Venter, J.H. O'Connell. *Nuclear Instruments and Methods in Physics Research B* **473** (2020) 43-47. <https://doi.org/10.1016/j.nimb.2020.04.004>
- [30] X. H. Huang, J. P. Tu, X. H. Xia, X. L. Wang, J. Y. Xiang, L. Zhang, Y. Zhou, *Journal of Power Sources* **188(2)** (2009) 588-591. <https://doi.org/10.1016/j.jpowsour.2008.11.111>
- [31] J. Zhao, Y. Tian, A. Liu, L. Song, Z. Zhao, *Materials Science in Semiconductor Processing* **96** (2019) 78-90. <https://doi.org/10.1016/j.mssp.2019.02.024>
- [32] H. Chen, H. Ma, H. Xia, Y. Chen, L. Zhang, *Optical Materials* **122** (2021) 111639. <https://doi.org/10.1016/j.optmat.2021.111639>
- [33] M. Velazquez-Rizo, P. Kirilenko, D. Iida, Z. Zhuang, K. Ohkawa, *Crystals* **12(2)** (2022) 211. <https://doi.org/10.3390/cryst12020211>

